ELSEVIER

Journal of Nuclear Materials 301 (2002) 15–22

journal of nuclear materials

www.elsevier.com/locate/jnucmat

Radiation effects in structural materials of spallation targets

P. Jung *

Institut für Festkörperforschung, Forschungszentrum Jülich, Association EURATOM-FZJ, D-52425 Jülich, Germany

Abstract

Effects of radiation damage by protons and neutrons in structural materials of spallation neutron sources are reviewed. Effects of atomic displacements, defect mobility and transmutation products, especially hydrogen and helium, on physical and mechanical properties are discussed. The most promising candidate materials (austenitic stainless steels, ferritic/martensitic steels and refractory alloys) are compared, and needed investigations are identified.

1. Introduction

Devices employing neutrons from spallation reactions of GeV-protons with high-Z target materials are under consideration for neutron scattering (SNS in USA, ESS in Europe), for waste transmutation (ADS in EU, AAA in USA), for energy production in sub-critical reactors (EA), and for tritium production. Systems combining several of the above applications are CONCERT in EU and JNS in Japan. Common to all of these current designs are liquid metal targets (Hg, PbBi, Pb) contained in metallic structures. Damaging of the structural materials results from irradiation by the energetic protons and neutrons which also may enhance the attack by the liquid metals and possibly other coolants. The present article gives an overview on the basic damaging processes as well as the resulting property changes. It concentrates on those metals which are most promising for spallation sources, i.e. austenitic and martensitic stainless steels and refractory alloys. As only very few experimental investigations have been performed in spallation environments, the selection of materials will largely depend on expertise acquired in previous material development programmes, e.g. for water-cooled reactors, high-temperature gas-cooled reactors, space power reactors, and mainly for fast breeders and fusion reactors.

2. Basic radiation damage processes

For applying those data to a spallation environment, the effects of the differences in particle spectra must be taken into account, especially the much higher energies of protons and neutrons involved. Basically three effects of irradiation on structural materials can be distinguished: structural changes from displacement and rearrangement of atoms, kinetic effects from enhanced redistribution of atoms by mobile defects with promotion of segregation and phase changes, and chemical changes from the production of new atomic species by nuclear reactions (transmutation).

2.1. Displacements

Cross sections for displacement σ_{dpa} are shown in Fig. 1 as a function of particle energy. It can be seen that above about 20 MeV the values for protons and neutrons become virtually equal and are only slightly increasing with energy. But at the higher energies the particles transfer higher energies T_p to the lattice atoms. This is sketched in Fig. 2, showing the integral fraction $W(T_p)$ of defects produced by primary knock-ons of energies up to T_p. At the lower side, the range of T_p is truncated by the threshold energy for defect production

* Tel.: +49-2461 614 036; fax: +49-2461 614 413.
E-mail address: p.jung@fz-juelich.de (P. Jung).

0022-3115/02/$ - see front matter
PII: S0022-3115(01)00722-X

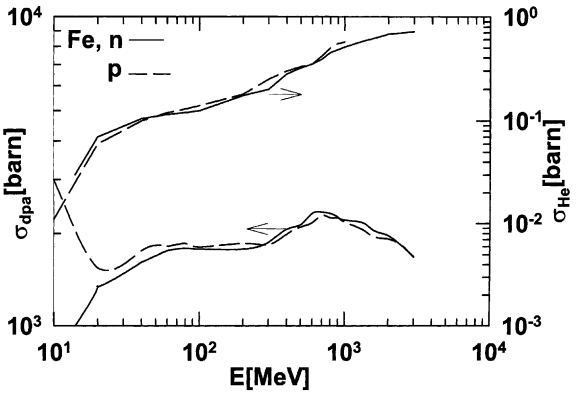

Fig. 1. Cross sections for production of displacement and helium in iron as a function of energy of protons and neutrons. The displacement cross sections are based on computer codes, while the helium cross sections are interpolations of experimental data as compiled in Ref. [1].

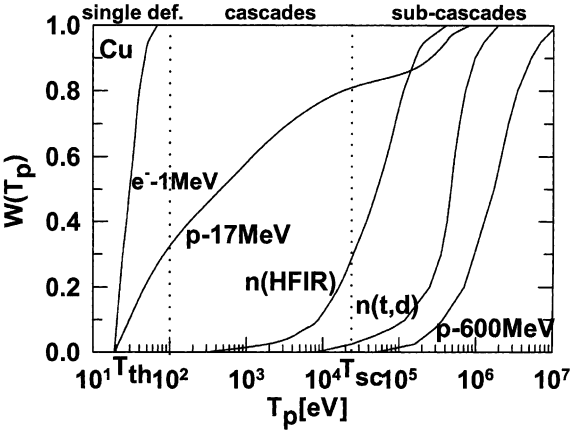

Fig. 2. Fraction $W(T_p)$ of defects produced by a primary knock-on of energy T_p. The range of T_p is truncated at the lower side by the threshold energy T_{th} for defect production, while on the upper side a maximum of T_p is given by the energy transferred in a head-on collision.

T_{th} (≈19 eV for Cu, cf. Ref. [2]), while on the upper side the maximum of T_p is given by the energy transferred in a head-on collision. It can be seen that the average recoil enegy for defect production is 50 keV for a fast reactor (e.g. HFIR), 500 keV for a (t,d)-fusion reactor, but 2 MeV for 600 MeV protons. For T_ps up to about 100 eV, the resulting defect structure consists mainly of single Frenkel defects, i.e. separate pairs of self-interstitials and vacancies. At higher energies defects are produced in cascades, with a core of vacancies surrounded by self-interstitals. The size of these cascades grows with increasing energy up to $T_p \approx 25$ keV where the cascades start to split up into clearly separated sub-cascades. This onset energy of sub-cascade formation (T_{sc}) increases with the mass of the target atoms [3–5]. This means that above T_{sc}, the defect structure is no longer changing qualitatively, but only the number of sub-cascades is increasing linearly with T_p. Therefore with respect to displacement damage, as derived from standard dpa calculations [6,7], the results from 14 MeV neutron irradiations could be adapted to the spallation environment with some confidence, while those from fast reactors only with some reserve. Also the integral displacement rates are not too different: <30 and ≈17 dpa/year in a fast breeder and fusion reactor (DEMO), respectively, compared to an estimated maximum of 50–100 dpa/year in the windows and target structures of ESS and ADS.

The basic products of atomic displacement are vacancies and self-interstitials and clusters thereof, the properties of which have been reviewed in Refs. [8–11]. Mutual encounters of equal or different types of these point defects due to thermally or irradiation induced migration and elastic interaction cause annihilation by recombination or clustering, respectively. These defects are also lost to sinks, e.g. cavities, dislocations, grain boundaries, surfaces etc., causing in turn also modifications of the sinks, e.g. growth of cavities (swelling) or dislocation loops, climb of dislocations (creep) etc. On the other hand clustering produces microvoids, stacking fault tetrahedra or dislocation loops, which may act as barriers to dislocations movement and eventually may cause hardening and embrittlement.

2.2. Radiation effects on diffusion, segregation and precipitation (RED, RIS, REP)

Thermal diffusion in metals proceeds by the vacancy mechanism. Aside from atomic mixing in cascades, the increased concentration of vacancies and the additional presence of self-interstitials causes so-called radiation enhanced diffusion (RED) [12]. In alloys RED varies for the different constituents due to their different interaction with defects, cf. Refs. [8,11,13]. The flux of defects to sinks gives rise to radiation induced segregation (RIS) or depletion by the coupled fluxes of the constituents [14,15], and, if solubility limits are exceeded, to radiation enhanced precipitation (REP) [16]. These effects are significant only in a dose-rate dependent temperature window, as exemplified schematically for RIS in Fig. 3. While at low homologous temperatures RIS is suppressed by recombination of defects, it is reduced at high temperatures by resolution. As a general rule, RIS seems to be largest for undersized atoms, while addition of oversized atoms may even suppress it. RIS and REP at grain boundaries can cause transgranular brittle fracture. Especially RIS can also have severe consequences on the interaction with the environment by promoting corrosion, stress corrosion cracking and liquid metal embrittlement.

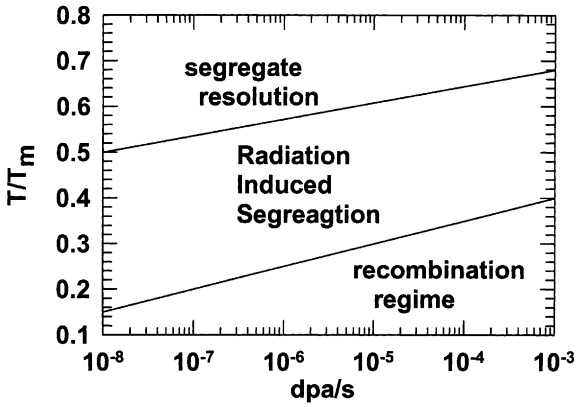

Fig. 3. Regime of homologous temperatures and dose rates in which radiation induced segregation RIS is most severe.

2.3. Transmutations

The production of new atomic species by transmutation may alter the absorption of neutrons, may induce radioactivity with consequences for service and waste disposal, and may change chemical composition and consecutively material properties. The production cross section are highest for the light transmutants hydrogen and helium, while the production of most other elements under fusion [17] as well as spallation conditions [18] will hardly exceed the solubility limits.

In contrast to the displacement cross section, the cross sections for helium production σ_α is continuously increasing with energy (Fig. 1), resulting in helium (and hydrogen) production rates for steels in spallation environments (estimated 0.5 at.% He/year in the windows of ESS, ADS) which are orders of magnitude above those encountered in fusion ($\approx$0.02 at.% He/year in DEMO) or fast fission (<0.0001 at.% He/year). For example the largest fusion devices of the next two generations will produce in their anticipated total lifetime only 0.004 (ITER) and 0.04 (DEMO) at.% He in steel, respectively. Negligible solubility and strong trapping of helium at the concurrently produced vacancies is well known and will lead to the buildup of considerable concentrations, cf. Refs. [13,19]. Helium can promote cavity nucleation and growth [20,21] and other microstructural changes [22]. Helium bubbles form in the matrix and at grain boundaries and grow at elevated temperatures already at concentrations below 100 at.ppm under the supply of vacancies, causing swelling and embrittlement. The production cross section for hydrogen is even about one order of magnitude higher than σ_α for $E > 10$ MeV. But there is hope that it has less effect on material degradation as a large fraction may be efficiently desorbed, due to its high mobility. On the other hand, there are indications that hydrogen is retained by irradiation defects, which needs further investigation [1].

These basic radiation effects and their superposition cause changes of physical and mechanical properties. At elevated temperatures, the only significant change of physical properties of structural alloys is reduction of density and associated dimensional changes (Chapter 3). Effects on other thermo-mechanical properties are small, e.g. thermal conductivity and thermal expansion. Concerning mechanical properties the most important effect is embrittlement, i.e. reduction of ductility and fracture toughness (Chapter 4), which is inherently related to radiation hardening. The most important parameters determining the amount of irradiation induced property changes in metallic materials are composition and temperature. Especially the difference in lattice structure between fcc (e.g. austenitic steels) and bcc (e.g. martensitic/ferritic steels) obviously significantly influences irradiation effects on virtually all properties. Fig. 4 shows a bar graph of the regimes of homologous temperature in which important properties of steels are most strongly affected by irradiation. Solid bars indicate those properties which are most severely affected in austenitic stainless steels, while dashed bars refer to martensitic/ferritic steels. The tentative operation regimes of ESS and ADS are also indicated. Already this very crude picture shows that for the operation of ESS at relatively low temperatures, austenitic stainless steel are most promising, while for the higher temperature in ADS, martensitic stainless steels might be advantageous. Data for refractories are yet insufficient to draw safe conclusions. The pulsed mode of irradiation, intended in ESS and unintentionally induced in ADS by team trips, will cause cyclic thermo-mechanical stresses. According to present knowledge those will not aggravate irradiation effects in comparison to steady state operation

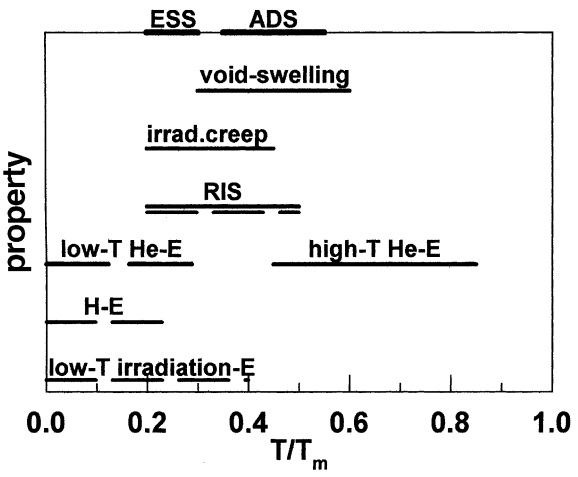

Fig. 4. Schematic view of ranges of homologous temperatures in which physical and mechanical properties of austenitic (solid) and martensitic (dashed) stainless steels are most seriously affected by irradiation (E stands for embrittlement).

[23], but in a liquid metal target may induce mechanical damage due to cavitation.

3. Dimensional changes

3.1. Swelling

The physical basis of swelling is an imbalance (bias) between interstitials and vacancies in production and/or in their loss to sinks, cf. Refs. [9–11]. During defect production in cascades, small glissile interstitial loops may be produced which can reach sinks, e.g. dislocations, by low-dimensional motion, leaving behind a surplus of vacancies (production bias [24]). Furthermore there is a net flux of self-interstitials to dislocations due to a stronger elastic attraction (annihilation bias [25]), while the excess vacancies tend to agglomerate to three-dimensional cavities. For reviews on physical basis and phenomenology of swelling see Refs. [11,26]. The occurrence of swelling is confined to a dose-rate dependent temperature window (Fig. 5), which resembles that for RIS in Fig. 3. At low temperatures the loss to sinks is impeded by recombination due to low mobility of the defects, while at high temperatures voids dissolve by the evaporation of vacancies. As a function of dose, volume change $\Delta V/V$ takes off at a very low rate up to an incubation dose Φt_S, and shows a linear dose dependence above:

$$\Delta V/V = S(\Phi t - \Phi t_S) \quad \text{for } \Phi t > \Phi t_S \tag{1}$$

For steels the transient dose Φt_S contains all dependencies on composition, gaseous impurities, pre-treatment (cold working), irradiation temperature, dose rate, etc., while the parameters S of linear swelling is apparently universal for a class of materials. Typical values of Φt_S for austenitic and martensitic stainless steels are 25 and >100 dpa, respectively, while the respective values of S in the regime of maximum swelling are 1 and 0.2%/dpa. The lower swelling in ferritic/martensitic steels has prompted a variety of possible explanations: differences in defect–sink interaction, binding of vacancies to interstitial impurities, enhanced recombination, screening of dislocations, etc. [29]. Swelling can be reduced by minor additions of P, Si, Ti, mainly by extending the incubation period. Saturation of swelling is observed only in materials which form void lattices [30]. Results on the effect of helium on void swelling are not yet conclusive, cf. Ref. [1]. In non-cubic metals which will not be treated here, dimensional changes also occur by irradiation growth, which is a shape change caused by preferential precipitation of self-interstitials and vacancies on planes of different orientations [31,32].

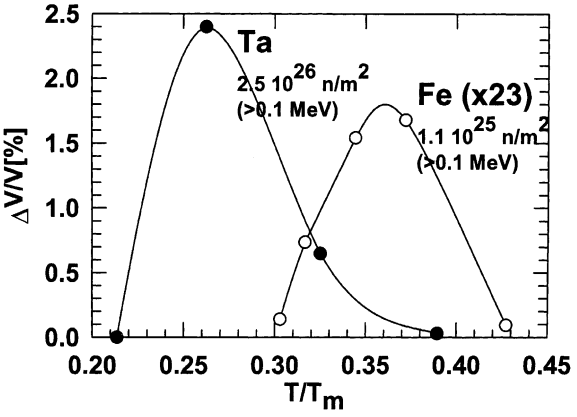

Fig. 5. Temperature dependence of swelling of tantalum [27] and iron [28] under neutron irradiation. For better comparison, data from iron data were multiplied by the ratio of neutron doses, assuming a linear dose dependence.

3.2. Effect of stress

Mechanical stresses affect the transient dose of swelling which is reduced under both, tension and compression [33]. Another possible cause of dimensional changes is volume conserving irradiation creep. It is driven by the dependence on stress direction of the interaction between interstitials and dislocations and, via the dependence on overall microstructure, also depends on the void population. Phenomenologically the corresponding length change can be described by

$$\Delta L/L = \Delta L/L_T + \sigma(B(\Phi t - \Phi t_T) + D\Delta V/V) \quad \text{for } \Phi_t > \Phi t_T, \tag{2}$$

where $\Delta L/L_T$ is a transient strain accumulated during a transient dose Φt_T, which dominates creep strain below about 200 °C. Similar to the case of swelling the irradiation creep rate, as described by the parameters B, is much higher in austenitic ($\approx 1 \times 10^{-6}$ Mpa^{-1} dpa^{-1}) than in ferritic/martensitic ($\approx 0.2 \times 10^{-6}$) stainless steels. On the other hand the dependence on swelling is similar for both ($D \approx 6 \times 10^{-3}$ Mpa^{-1}). At high stresses a more than linear stress dependence is observed which is ascribed to contribution of dislocation glide [34]. Irradiation creep may to some degree be beneficial, as it can relieve internal stresses or stress concentrations, which may result for example from differential swelling. Results on effects of hydrogen or helium content on irradiation creep are not available.

4. Embrittlement

The most detrimental effect of irradiation on structural materials is loss of ductility, and/or reduction of

fracture toughness, often associated with a change of fracture mode from ductile (dimple, transgranular) to brittle (cleavage or intergranular). This embrittlement by irradiation is often combined with hardening, which by itself would mostly be a desirable effect. The appearance of embrittlement depends on the modes of mechanical loading, which are experienced, separately or in combination, by the materials in a spallation target: constant tensile or compressive stresses, impacts from pressure waves in the liquid metal, and fatigue loading from unavoidable frequent beam trips or from the high-cycle pulsed operation in ESS. Fracture behaviour also depends on specimen shape. Below a certain limit of thicknesses, target structures or test specimens are in the transition region between plain-stress and plain-strain conditions, giving higher fracture toughness than in bulk material. This has to be taken into account, when for example data from miniature specimens in irradiation experiments are applied [35]. Sections 4.1–4.4 detail processes which induce embrittlement.

4.1. Irradiation embrittlement

Most metallic materials experience increase of hardness and strength and reduction of plastic strain under irradiation. This is most probably due to pinning of dislocations by irradiation induced dislocation loops, precipitates, cavities or bubbles. Mostly more than one of these types of defects are produced, which makes it difficult to precisely assess their relative contribution. In Fig. 6 uniform elongations ε_U of austenitic 316L and martensitic F82H are plotted as a function of irradiation dose for high-energy protons (solid) and fast neutrons (dashed). Due to differences in temperatures, comparison of data from both environments is not clear, but in all cases ε_U tends to saturate at doses of a few dpa. Furthermore at higher doses the precise determination of ε_U is difficult as both these steels show a yield point and subsequent continuous decrease of flow stress until fracture [36,38]. In the case of proton data, the contributions from hydrogen and helium (see Sections 4.2 and 4.3) have to be sorted out, in order to determine the peculiar contribution from displacements.

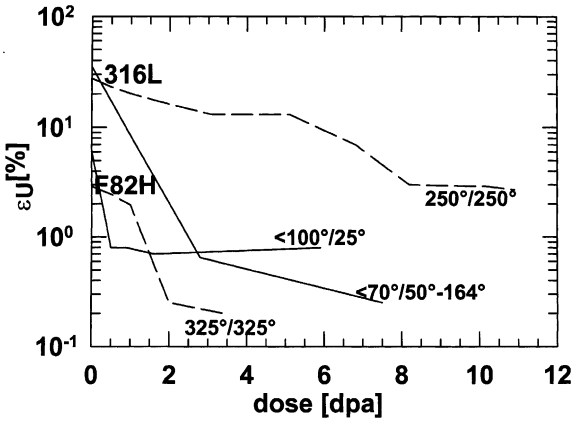

Fig. 6. Dose dependence of uniform elongation ε_U of austenitic 316L [36,37] and martensitic F82H [38,39] after irradiation with high-energy protons (—) and fast neutrons (- - -). Irradiation and test temperatures are indicated on each curve.

Low-cycle fatigue tests after fast neutron irradiation of AISI316 to 5 dpa showed a slightly reduced fatigue life at 500 °C, which was further reduced at 10 dpa and 600–700 °C. On the other hand lifetime was increased by irradiation in the regime of high-cycle fatigue ($>10^5$ cycles) which is ascribed to hardening [40]. After irradiation in a mixed spectrum reactor to 9–15 dpa which simultaneously produces 400–820 at.ppm He, some reduction of fatigue life was also observed at 430 °C, while virtually no change was found at 550 °C [41].

4.2. Hydrogen embrittlement

In spite of the large amount of hydrogen produced by energetic protons and neutrons (typically ≈1 at.% at 10 dpa), it probably will make only a minor contribution to the reduction of ductility in Fig. 6, as a significant fraction is lost by evaporation through the surfaces. Nevertheless, embrittlement by hydrogen is a well known phenomenon in steels, especially martensitic/ferritics, and is ascribed to a variety of mechanism, with embrittlement mostly increasing with decreasing strain rate, cf. Ref. [42]. Hydrogen may be present in spallation or other nuclear devices also from radiolysis if water cooling is involved, or from hydrogen used as a corrosion inhibitor. These sources of hydrogen might be blocked by permeation barriers, while this is not possible for hydrogen produced by transmutation. An assessment of the risk of hydrogen embrittlement is extremely difficult as many variables are important [43]. Only limited information on effects of irradiation on hydrogen retention is available. Hydrogen implanted at room temperature reduces the uniform elongation of low-activation martensitic stainless steel at ambient from about 5 to an apparently saturating at about 2.5% at concentrations above 0.14 at.%, while this embrittlement decreases with increasing temperature [1]. Synergy effects of irradiation and hydrogen on embrittlement have been found in tensile tests on 9Cr–2W steel. Neutron irradiation plus hydrogen loading caused much stronger embrittlement than irradiation or H alone [44,1].

Under fatigue conditions, crack growth per cycle is enhanced by hydrogen [45] and the number of cycles to failure is reduced [46]. Both effects are strongest at low frequencies and the latter is further enhanced by holding times. Nevertheless absolute crack growth rates are

lower at the low frequencies, and effects of frequency and holding time on total lifetime cannot clearly be discerned.

4.3. Helium embrittlement

Embrittlement by helium at high temperatures was already considered in the fast breeder material programmes and became of even more serious concern for fusion reactors. For a review on experiments and theories cf. Refs. [47–49]. The basic reason for the strong reduction of strain to failure and lifetime observed under constant stress in helium doped austenitic stainless steels, and even more in Ni-base alloys, are bubbles which form at grain boundaries. The embrittlement can be reduced by addition of titanium which supplies traps for helium by carbide precipitation. The resistance of martensitic/ferritic steels to helium embrittlement can similarly be ascribed to a large number of microstructural traps and in addition to a lower effective stress at the grain boundaries due to lower matrix strength [47]. Recently, impact tests on martensitic steels, containing up to 300 at.ppm helium from implantation [50] or from boron doping [51,52], showed embrittlement close to ambient (low temperature helium embrittlement). On the other hand tensile tests showed no embrittlement of martensitic steels up to 500 at.ppm He [53], but strong embrittlement at 5000 at.ppm [54] (Fig. 7). This may indicate that low embrittlement by helium at low temperatures is more severe at high strain rates, e.g. impact tests. Austentitic 316L was embrittled at room temperature only above 0.5 at.% He [55].

As in the case of hydrogen, reduction of the number of cycles to failure (and of lifetime) of austenitic stainless steels at elevated temperatures (600 °C) by preimplanted helium is most pronounced at low frequencies ($<\approx 1/s$) [56]. In martensitic steels, helium produced by implantation [57] or transmutation [58], had only a minor effect on fatigue lifetime in tests performed during irradiation, while some reduction was observed in post-irradiation tests.

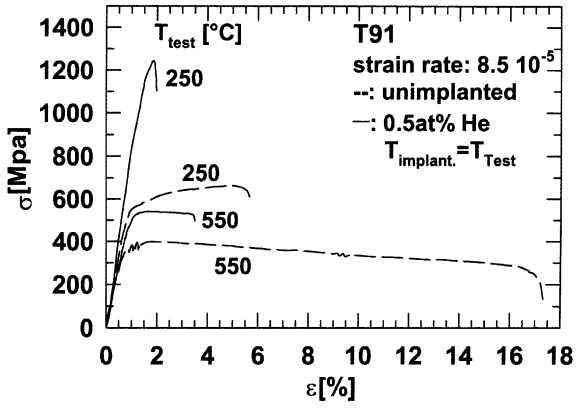

Fig. 7. Effect of 0.5 at.% helium, implanted at 250 or 550 °C into martensitic T91 on tensile curves recorded at the implantation temperature [52].

4.4. Environmental embrittlement (IASCC, LME)

The corroding and embrittling effects of the liquid metal target on the structural materials in a spallation source (and in addition by the cooling water in the ESS design) can be aggravated by simultaneous irradiation. The three prerequisites of stress corrosion cracking are a corrosive medium (e.g. water), a susceptible material and a tensile stress component. Irradiation can act on all of these three factors by making the liquid more aggressive due to radiolysis, by sensitising the material by RIS, and by producing additional stresses, for example by differential swelling. This so-called irradiation assisted stress corrosion cracking (IASCC) is well known from light water reactors (LWR). In Fig. 8 the intergranular stress corrosion cracking of 304 stainless steel in oxygenated water is plotted as a function of chromium concentration at grain boundaries. While the data points compile results after irradiation in LWRs, the lines indicate results from material, sensitised by annealing, cf. Ref. [13]. The similarity of both results

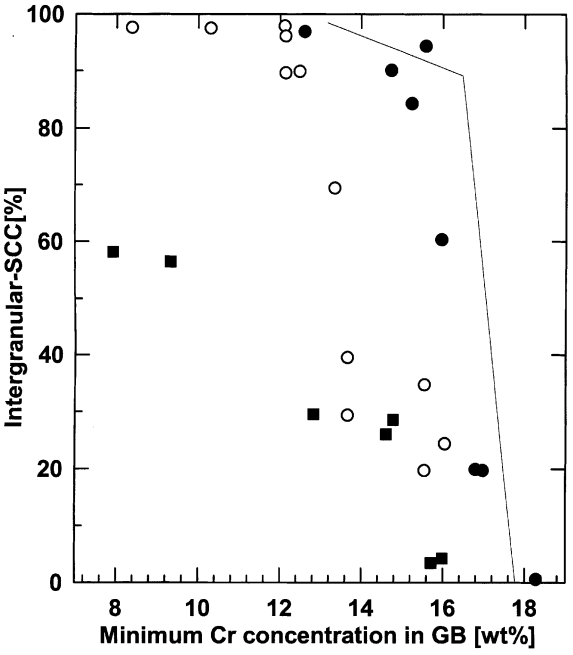

Fig. 8. Intergranular stress corrosion cracking of 304 stainless steel, irradiated in oxygenated water as a function of chromium concentration at grain boundaries as compiled in Ref. [13]. The line indicates results from material, sensitised by annealing.

indicates that the underlying mechanism is probably the same, namely depletion of chromium from grain boundaries by RIS and precipitation of Cr-rich $M_{23}C_6$, respectively. Additional contributions to embrittlement from hydrogen (Section 4.2), produced by radiolysis, is suspected.

Corrosion and embrittlement by liquid metals (LME) are complex phenomena and almost every liquid–solid couple behaves differently, for references. see Ref. [59]. In addition the attack of liquid metals is strongly affected by the dissolution or cracking of surface layers (e.g. oxides). Also subsequent selective leaching of alloy components strongly depends on composition. With respect to corrosion of stainless steels, a systematic study has shown, that weight loss in liquid Hg shows a shallow minimum around an alloying content (Cr + Ni + Mo) around 10% and then strongly increases, giving the martensitic steels a clear bonus compared to austenitics [60]. For the occurrence of severe LME some general rules (necessary but not sufficient) have been established: (1) low solubility of the solid in the liquid metal and vice versa, (2) no formation of intermetallic compound and (3) low corrosion rate. This means there is some antagonism between LM-corrosion and LME. Under fatigue loading, a constructional steel (AISI4340) showed strong reduction of cycles to failure by Hg coating in the high-cycle regime [61]. All these results refer to the case without irradiation, while only in alkali-metals tests under irradiation conditions have been performed in the fast breeder programmes.

5. Conclusions

1. Displacement damage in a spallation environment is qualitatively similar to that under (*t*,*d*) fusion, but transmutation (e.g. production of H, He) is much higher.
2. These high production rates of light elements will finally limit the lifetime of structural materials in the spallation target area.
3. Most irradiation effects give austenitic stainless steels an advantage at lower and martensitics at higher temperatures, respectively.
4. Fracture toughness, also under irradiation, might be improved by control of the content of minor alloying elements or impurities.
5. Investigations on corrosion and embrittlement by liquid metals under irradiation are most urgently needed. A first step could be tests without irradiation on appropriately pre-irradiated or implanted specimens, e.g. from spent spallation targets.
6. As the target will unavoidably have to be replaced regularly, material development has to proceed also after the decisions on the first design, to improve performance, lifetime and safety.

References

[1] P. Jung, C. Liu, J. Chen, J. Nucl. Mater. 296 (2001) 165.
[2] P. Jung, in: H. Ullmaier (Ed.), Landolt–Börnstein New Series, vol. III/25, Springer, Berlin, 1991, p. 1.
[3] M. Kiritani, T. Yoshiie, S. Kojima, Y. Satoh, Radiat. Eff. Defects Solids 113 (1990) 75.
[4] H.L. Heinisch, B.N. Singh, Philos. Mag. A 67 (1992) 407.
[5] K.L. Merkle, in: N.L. Petersen, S.D. Harkness (Eds.), Radiation Damage in Metals, American Society for Metals, Metals Park, OH, 1976, p. 75.
[6] M.J. Norgett, M.T. Robinson, I.M. Torrens, Nucl. Eng. Des. 33 (1975) 50.
[7] ASTM Standard Designation: E 521-83, vol. 12.02, 1983, p. 233.
[8] P. Ehrhart, H. Schultz, in: H. Ullmaier (Ed.), Landolt–Börnstein New Series, vol. III/25, Springer, Berlin, 1991, p. 88.
[9] W. Schilling, H. Ullmaier, in: R.W. Cahn, P. Haasen, E.J. Kramer (Eds.), Material Science and Technology, in: B.R.T. Frost (Ed.), Nuclear Materials, Part 2, vol. 10B, VCH, Weinheim, 1994, p. 179.
[10] H. Ullmaier, H. Trinkaus, in: Physical Processes of the Interaction of Fusion Plasmas with Solids, Academic Press, New York, 1996, p. 305.
[11] H.J. Wollenberger, in: R.W. Cahn, P. Haasen (Eds.), Physical Metallurgy, 4th Ed., vol. II, Elsevier, Amsterdam, 1996, p. 1621.
[12] H. Wollenberger, V. Naundorf, M.-P. Macht, in: R.P. Agarwala (Ed.), Diffusion Processes in Nuclear Materials, Elsevier, Amsterdam, 1992, p. 201.
[13] P. Jung, Met. Mater. Proc. (India) 11 (1999) 191.
[14] H. Wiedersich, N.Q. Lam, in: F.V. Nolfi (Ed.), Phase Transformation During Irradiation, Applied Science, London, 1983, p. 1.
[15] L.E. Rehn, P.R. Okamoto, in: F.V. Nolfi (Ed.), Phase Transformation During Irradiation, Applied Science, London, 1983, p. 247.
[16] K.C. Russell, J. Nucl. Mater. 206 (1993) 129.
[17] D.G. Doran, F.M. Mann, L.R. Greenwood, J. Nucl. Mater. 174 (1990) 125.
[18] G. Küppers, J. Radioanal. Nucl. Chem. 218 (1997) 183.
[19] H. Ullmaier, in: H. Ullmaier (Ed.), Landolt–Börnstein New Series, vol. III/25, Springer, Berlin, 1991, p. 380.
[20] L.K. Mansur, W.A. Coghlan, J. Nucl. Mater. 119 (1983) 1.
[21] L.K. Mansur, E.H. Lee, P.J. Maziasz, A.P. Rowcliffe, J. Nucl. Mater. 141–143 (1986) 633.
[22] D.F. Pedraza, P.J. Maziasz, R.L. Klueh, Radiat. Eff. Def. Solids 113 (1990) 213.
[23] H. Trinkaus, J. Nucl. Mater. 296 (2001) 101.
[24] G.W. Greenwood, A.J.E. Foreman, D.E. Rimmer, J. Nucl. Mater. 4 (1959) 305.
[25] H. Trinkaus, B.N. Singh, C.H. Woo, J. Nucl. Mater. 212–215 (1994) 18.
[26] F.A. Garner, in: R.W. Cahn, P. Haasen, E.J. Kramer (Eds.), Material Science and Technology, in: B.R.T. Frost (Ed.), Nuclear Materials, Part 2, vol. 10B, VCH, Weinheim, 1994, p. 419.
[27] F.W. Wiffen, J. Nucl. Mater. 67 (1977) 119.
[28] L.L. Horton, J. Bentley, K. Farrell, J. Nucl. Mater. 108&109 (1982) 222.

[29] A. Almazouzi, T. Diaz de la Rubia, B.N. Singh, M. Victoria, J. Nucl. Mater. 276 (2000) 295.
[30] K. Krishan, Radiat. Eff. 66 (1982) 121.
[31] V. Fidleris, J. Nucl. Mater. 158 (1988) 22.
[32] R.A. Holt, J. Nucl. Mater. 158 (1988) 310.
[33] H.K. Sahu, P. Jung, J. Nucl. Mater. 136 (1985) 154.
[34] L.K. Mansur, in: G.R. Freeman (Ed.), Kinetics of Non-homogeneous Processes, Wiley-Interscience, New York, 1988, p. 377.
[35] P. Jung, A. Hishinuma, G.E. Lucas, H. Ullmaier, J. Nucl. Mater. 232 (1996) 186.
[36] S. Maloy, Report Los Alamos Nat. Lab., TPO-E71-TRT-X-00079, LA-UR-99-1673, 1999.
[37] J.D. Elen, P. Fenici, J. Nucl. Mater. 191–194 (1992) 766.
[38] Y. Dai, S.A. Maloy, G.S. Bauer, W.F. Sommer, J. Nucl. Mater. 283–287 (2000) 513.
[39] A. Alamo, Report CEA, NT SRMA 00-2395, 2000.
[40] D.J. Michel, H.H. Smith, in: M.L. Bleiberg, J.W. Bennett (Eds.), Radiation Effects in Breeder Reactor Structural Materials, The Metallurgical Society of AIME, New York, 1977, p. 117.
[41] M.L. Grossbeck, K.C. Liu, J. Nucl. Mater. 103&104 (1981) 853.
[42] J.P. Hirth, Metall. Trans. A 11 (1980) 861.
[43] G. Nelson, in: M.R. Louthan, R.P. McNitt, R.D. Sisson (Eds.), Proceedings of the Conference on Environmental Degradation of Engineering Materials III, Pennsylvania State University, 1987, p. 83.
[44] A. Kimura, H. Kayano, M. Narui, J. Nucl. Mater. 179–181 (1991) 737.
[45] G.F. Rodney, R.H. Jones, J. Nucl. Mater. 155–157 (1988) 760.
[46] J.I. Shakib, H. Ullmaier, E.A. Little, R.G. Faulkner, W. Schmitz, T.E. Chung, J. Nucl. Mater. 212–215 (1994) 579.
[47] H. Schroeder, U. Stamm, ASTM STP 1046 (1989) 223.
[48] H. Trinkaus, Radiat. Eff. 101 (1986) 91.
[49] H. Ullmaier, H. Trinkaus, Mater. Sci. Forum 97–99 (1992) 451.
[50] R. Lindau, A. Möslang, D. Preininger, M. Rieth, H.D. Röhrig, J. Nucl. Mater. 271&272 (1999) 450.
[51] R.L. Klueh, D.J. Alexander, J. Nucl. Mater. 218 (1995) 151.
[52] M. Rieth, B. Dafferner, H.D. Röhrig, J. Nucl. Mater. 233–237 (1996) 351.
[53] K.K. Bae, K. Ehrlich, A. Möslang, J. Nucl. Mater. 191–194 (1992) 905.
[54] P. Jung, J. Henry, et al., unpublished.
[55] H. Ullmaier, E. Camus, J. Nucl. Mater. 251 (1997) 262.
[56] L.S. Batra, H. Ullmaier, K. Sonnenberg, J. Nucl. Mater. 116 (1983) 136.
[57] R. Lindau, A. Möslang, J. Nucl. Mater. 212–215 (1994) 594.
[58] P. Marmy, J. Nucl. Mater. 212–215 (1994) 594.
[59] N.S. Stoloff, in: M.H. Kamdar (Eds.), Embrittlement by Liquid and Solid Metals, Metallurgical Society of AIME, New York, 1984.
[60] J.F. Nejedlik, E.J. Vargo, Corrosion 20 (1964) 384.
[61] D.W. Levinson, L.E. Tanner, J.J. Rausch, Armour Research Foundation, unpublished.